Animal treatment

At least 3 mice between 8 and 10 weeks old were used for each treatment. Mice were pretreated by intraperitoneal injection with corn oil, PB (100 mg per kg body weight, Sigma) or TCPOBOP (3 mg per kg body weight, a gift from S. Safe) for indicated time. For 3-day PB treatment, mice were injected intraperitoneally three times with PB, one injection per day.

Zoxazolamine paralysis test

Mice pretreated with corn oil, PB or TCPOBOP were given a single intraperitoneal injection of zoxazolamine (300 mg per kg body weight, Sigma), 24 h after the last dose of PB. Mice were placed on their backs and paralysis time was defined as the time required for the animal to regain sufficient consciousness to right itself repeatedly[22].

Cocaine treatment and ALT assay

Male mice pretreated with corn oil, PB or TCPOBOP were injected intraperitoneally with cocaine HCl (30 mg per kg body weight), 24 h after the last injection of PB. The mice were anaesthetized 22 h after cocaine treatment. Blood was drawn from the eye for determination of serum alanine aminotransferase (ALT) activity. ALT activity was determined using *Vitros* ALT slides (Johnson & Johnson Clinical Diagnostics). The procedure was performed at the Methodist Hospital in Houston.

RNA analysis

20 μg of total RNA from individual mouse livers was subjected to northern blot analysis. A mouse CAR complementary DNA probe was used to reveal the absence of CAR transcripts in the CAR null mice. Probes for Cyp2b10 were prepared by polymerase chain reaction after reverse transcription of RNA (RT-PCR) with mouse liver total RNA using Super-script One-step RT-PCR System (Life Technologies). PCR primers were 5′-CCGCCTC TAGAAGTCAACATTGGTTAGAC-3′ and 5′-CCGCCGGATCCCACACTAAGCCTCAT AAT-3′.

Determination of hepatocyte proliferation following PB or TCPOBOP treatment

Mice pretreated with corn oil, PB or TCPOBOP received a single intraperitoneal dose of BrdU/FdU (2 ml per 100 g body weight, Amersham). Mice were killed 2 h after BrdU administration. BrdU incorporation was determined using a mouse anti-BrdU monoclonal antibody (DAKO) and Vectastain ABC Kit (Vector Laboratories).

1. Waxman, D. J. P450 gene induction by structurally diverse xenochemicals: central role of nuclear receptors CAR, PXR, and PPAR. *Arch. Biochem. Biophys.* **369**, 11–23 (1999).
2. Poland, A. *et al.* 1,4-Bis[2-(3,5-dichloropyridyloxy)]benzene, a potent phenobarbital-like inducer of microsomal monooxygenase activity. *Mol. Pharmacol.* **18**, 571–580 (1980).
3. Honkakoski, P., Zelko, I., Sueyoshi, T. & Negishi, M. The nuclear orphan receptor CAR-retinoid X receptor heterodimer activates the phenobarbital-responsive enhancer module of the CYP2B gene. *Mol. Cell. Biol.* **18**, 5652–5658 (1998).
4. Sueyoshi, T., Kawamoto, T., Zelko, I., Honkakoski, P. & Negishi, M. The repressed nuclear receptor CAR responds to phenobarbital in activating the human CYP2B6 gene. *J. Biol. Chem.* **274**, 6043–6046 (1999).
5. Tzameli, I., Pissios, P., Schuetz, E. G. & D, Moore, D. D. The xenobiotic compound 1,4-bis[2-(3,5-dichloropyridyloxy)]benzene is an agonist ligand for the nuclear receptor CAR. *Mol. Cell. Biol.* **20**, 2951–2958 (2000).
6. Jones, S. A. *et al.* The pregnane X receptor: a promiscuous xenobiotic receptor that has diverged during evolution. *Mol. Endocrinol.* **14**, 27–39 (2000).
7. Moore, L. B. *et al.* Orphan nuclear receptors, constitutive androstane receptor and pregnane X receptor share xenobiotic and steroid ligands. *J. Biol. Chem.* **275**, 15122–15127 (2000).
8. Baes, M. *et al.* A new orphan member of the nuclear receptor superfamily that interacts with a subset of retinoic acid response elements. *Mol. Cell. Biol.* **14**, 1544–1552 (1994).
9. Choi, H. S. *et al.* Differential transactivation by two isoforms of the orphan nuclear hormone receptor CAR. *J. Biol. Chem.* **272**, 23565–23571 (1997).
10. Heubel, F., Reuter, T. & Gerstner, E. Differences between induction effects of 1,4-bis[2-(3,5-dichloropyridyloxy)]benzene and phenobarbitone. *Biochem. Pharmacol.* **38**, 1293–1300 (1989).
11. Carthew, P., Edwards, R. E. & Nolan, B. M. The quantitative distinction of hyperplasia from hypertrophy in hepatomegaly induced in the rat liver by phenobarbital. *Toxicol. Sci.* **44**, 46–51 (1998).
12. Cunningham, M. L. Role of increased DNA replication in the carcinogenic risk of nonmutagenic chemical carcinogens. *Mutat. Res.* **365**, 59–69 (1996).
13. Robinson, J. R. & Nebert, D. W. Genetic expression of aryl hydrocarbon hydroxylase induction. Presence or absence of association with zoxazolamine, diphenylhydantoin, and hexobarbital metabolism. *Mol. Pharmacol.* **10**, 484–493 (1974).
14. Bornheim, L. M. Effect of cytochrome P450 inducers on cocaine-mediated hepatotoxicity. *Toxicol. Appl. Pharmacol.* **150**, 158–165 (1998).
15. Kliewer, S. A. *et al.* An orphan nuclear receptor activated by pregnanes defines a novel steroid signaling pathway. *Cell* **92**, 73–82 (1998).
16. Blumberg, B. *et al.* SXR, a novel steroid and xenobiotic-sensing nuclear receptor. *Genes Dev.* **12**, 3195–3205 (1998).
17. Lehmann, J. M. *et al.* The human orphan nuclear receptor PXR is activated by compounds that regulate CYP3A4 gene expression and cause drug interactions. *J. Clin. Invest.* **102**, 1016–1023 (1998).
18. Xie, W. *et al.* Humanized xenobiotic response in mice expressing nuclear receptor SXR. *Nature* **406**, 435–439 (2000).
19. Shimada, T., Yamazaki, H., Mimura, M., Inui, Y. & Guengerich, F. P. Interindividual variations in human liver cytochrome P-450 enzymes involved in the oxidation of drugs, carcinogens and toxic chemicals: studies with liver microsomes of 30 Japanese and 30 Caucasians. *J. Pharmacol. Exp. Ther.* **270**, 414–423 (1994).
20. Code, E. L. *et al.* Human cytochrome P4502B6: interindividual hepatic expression, substrate specificity, and role in procarcinogen activation. *Drug Metab. Dispos.* **25**, 985–993 (1997).
21. Selim, K. & Kaplowitz, N. Hepatoxicity of psychotropic drugs. *Hepatology* **29**, 1347–1351 (1999).
22. Liang, H. C. *et al.* Cyp1a2(−/−) null mutant mice develop normally but show deficient drug metabolism. *Proc. Natl Acad. Sci. USA* **93**, 1671–1676 (1996).

Structure of a serpin–protease complex shows inhibition by deformation

James A. Huntington, Randy J. Read & Robin W. Carrell

Department of Haematology, University of Cambridge, Wellcome Trust Centre for Molecular Mechanisms in Disease, Cambridge Institute for Medical Research, Hills Road, Cambridge CB2 2XY, UK

The serpins have evolved to be the predominant family of serine-protease inhibitors in man[1,2]. Their unique mechanism of inhibition involves a profound change in conformation[3], although the nature and significance of this change has been controversial. Here we report the crystallographic structure of a typical serpin–protease complex and show the mechanism of inhibition. The conformational change is initiated by reaction of the active serine of the protease with the reactive centre of the serpin. This cleaves the reactive centre, which then moves 71 Å to the opposite pole of the serpin, taking the tethered protease with it. The tight linkage of the two molecules and resulting overlap of their structures does not affect the hyperstable serpin, but causes a surprising 37% loss of structure in the protease. This is induced by the plucking of the serine from its active site, together with breakage of interactions formed during zymogen activation[4]. The disruption of the catalytic site prevents the release of the protease from the complex, and the structural disorder allows its proteolytic destruction[5,6]. It is this ability of the conformational mechanism to crush as well as inhibit proteases that provides the serpins with their selective advantage.

The irreversibility of inhibition achieved by the serpins has made them the principal inhibitors controlling both intra- and extracellular proteolytic pathways. In human plasma, antithrombin controls coagulation, C1-inhibitor controls complement activation, and the inhibitors of plasmin and its activators control fibrinolysis. To determine the structural basis of the serpin mechanism we chose another of the plasma serpins, the archetypal member of the family, α1-antitrypsin[7,8]. There have been many unsuccessful attempts over the past 20 years to crystallize the serpin–protease complex. Although the half-life of the complex in isolation is of the order of years, the extreme proteolytic susceptibility of the complex coupled with the high concentrations required for protein crystallization result in a level of heterogeneity incompatible with crystal growth. To overcome these difficulties, we purified the complex from a reaction mixture containing an excess of α1-antitrypsin over trypsin, and set up crystallization trials at 4 °C. Crystals were obtained within two weeks, and SDS–polyacrylamide gel electrophoresis of an isolated crystal at the time of data collection confirmed it contained only intact complex (see Supplementary Information). The crystal structure at 2.6 Å resolution clearly shows
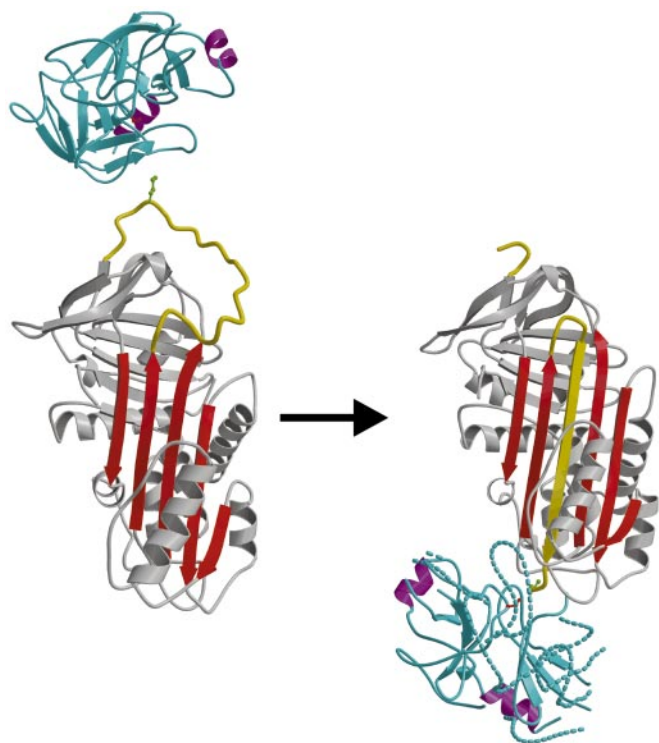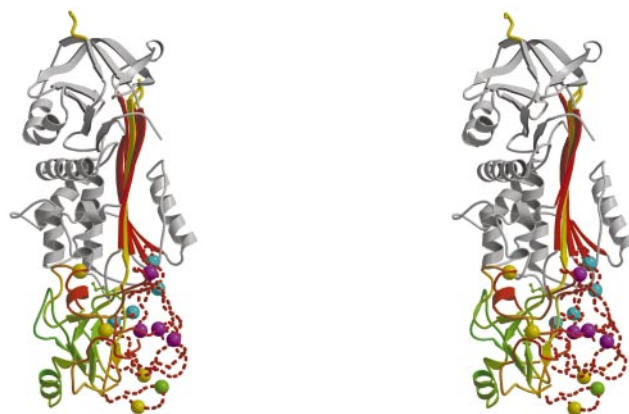
Figure 1 Formation of the complex. Ribbon depictions of native α_1-antitrypsin[8] with trypsin aligned above it in the docking orientation (left), and of the complex showing the 71 Å shift of the P1 methionine of α_1-antitrypsin, with full insertion of the cleaved reactive-centre loop into the A-sheet (right). Regions of disordered structure in the complexed trypsin are shown as interrupted coils projected from the native structure of trypsin. Red, α_1-antitrypsin β-sheet A; yellow, reactive-centre loop; green ball-and-stick, P1 Met; cyan, trypsin (with helices in magenta for orientation); red ball-and-stick, active serine 195.

Figure 2 Proteolytic susceptibility of the complexed protease. A stereo side view of the complex coloured according to Cα temperature factors for trypsin (α_1-antitrypsin, coloured as in Fig. 1, retains the low B-factors of its isolated cleaved form). The nine sites of proteolytic cleavage are shown as balls and all occur in regions of crystallographic disorder or high mobility. Cleavage sites: green, of trypsin, by trypsin[5]; yellow, of chymotrypsin, by chymotrypsin[6]; magenta, of chymotrypsin, by neutrophil elastase[6]. Temperature factors from blue to red, going through green at 40 Å^2, yellow at 60 Å^2 and red at 90 Å^2. When the full native trypsin structure is superimposed on the ordered region of trypsin in the complex there are no clashes with symmetry related molecules. The only significant steric overlap is within the asymmetric unit between the serpin and the disordered region of trypsin, as denoted here by cyan balls.

the unique mechanism of inhibition used by the serpins. Figure 1 shows the formation of the complex; Fig. 2 shows the distortion of the protease and explains its increased susceptibility to proteolysis; Fig. 3 shows the ester bond between the serpin and the protease, and the disruption of the protease active site. Other figures showing the electron density are available as Supplementary Information.

A glance at the structures in Fig. 1 immediately answers a much-debated question in the field. Wright and Scarsdale[9] proposed that inhibition involved insertion of the cleaved reactive-centre loop of the serpin into the A β-sheet of the molecule, with a pole-to-pole displacement of the protease. There has however been disagreement as to the extent of loop insertion, with conflicting evidence for both full[10,11] and partial[12] insertion. Here we see that there is full incorporation of the reactive-centre loop, from its hinge region to the reactive-centre Met 358 (denoted P15–P1). Indeed, the conformation of α_1-antitrypsin in the complex is precisely superimposable with that of the structure of isolated cleaved α_1-antitrypsin[3] (r.m.s. deviation 0.52 Å for all Cα atoms). This structure[3] was the starting point for subsequent deductions that the serpins were metastable proteins[13] with a mobile reactive-centre loop[14] and a spring-like inhibitory mechanism[9,15]. A more recent serpin structure[16] has shown how initial insertion of the first four residues of the loop (P15–P12) can take place, at which stage the F-helix appears likely to impede further movement of the bulky protease along the sheet. However, Fig. 2 shows how the protease could readily skirt the protuberant F-helix to reach its final position somewhat skew of the central axis of the serpin.

The unexpected finding from the structure of the complex is the degree of conformational disorder induced in the protease. Trypsin is a typical member of the chymotrypsin family and has a well

conserved, stable structure that is resistant to proteolysis. That perturbation could occur in the complexed trypsin was predicted from previous studies[5,6,17] showing a loss of stability and an increase in proteolytic vulnerability of proteases in complexes with serpins. But the surprise is the extent of the disruption observed here, such that although clear and continuous density was seen for more than 60% of the structure of trypsin, some 37% was crystallographically disordered (missing residues 16–41, 62–84, 110–120, 139–156, 186–190, 223–224). The presence within this disordered region of all the previously identified sites of proteolytic cleavage (Fig. 2) is evidence that the disorder represents the changes occurring *in vivo*. The ability to partially denature their cognate proteases is unique to the serpins, and the advantage it gives in making the complex more susceptible to clearance and degradation further explains the biological success of this family. One enzyme that efficiently cleaves complexed proteases[6] is neutrophil elastase, which is present in high concentrations in inflammatory loci. Such cleavage of the protease in the complex will be of physiological advantage, as it allows localized destruction of the protease before the slower receptor-based uptake of the serpin–protease complex from the circulation.

What is the explanation for the unusual stability of the serpin–protease complex? As compared with the other families of serine protease inhibitors, the complexes of proteases with serpins can persist for months or even years *in vitro*[18]. Does the acyl-protease intermediate persist as the result of the exclusion of water, required for hydrolysis, from the active site of trypsin, or is there a distortion of the active site that prevents catalytic deacylation? The structure clearly excludes the first of these possibilities, as the degree of crystallographic disorder, and hence of structural mobility, in the region adjacent to the active site is incompatible with the exclusion of water from the site. Nonetheless, no ordered water molecule is observed in the vicinity of the ester bond or the catalytic His 57. As Fig. 3 shows, there is a gross distortion of the catalytic site of the trypsin with a movement of Ser 195 to a position more than 6 Å away from its catalytic partner His 57. This is well beyond the proximity required for catalytic deacylation, and furthermore the movement of the serine effectively destroys the adjacent oxyanion hole (N–H of Gly 193 and Ser 195) required for the stabilization of
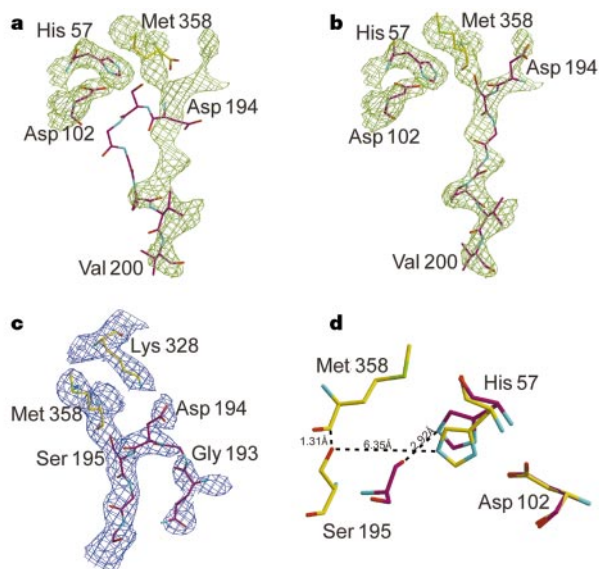
Figure 3 Disruption of active site. The ester bond and distortion of the active site of trypsin is evident from the initial map calculated from the molecular replacement solution of α_1-antitrypsin (green) shown with the initial (**a**) and final (**b**) models of trypsin and P1 Met 358. **c**, The refined electron density (blue) shows the stretching of the active-site loop resulting in the loss of the oxyanion hole and the replacement of the stabilizing 'activation' salt-bridge between the N-terminal amine and Asp 194 of trypsin with Lys 328 of α_1-antitrypsin. **d**, The catalytic triad of native trypsin (magenta) is grossly distorted in the complex (yellow) with a shift of Ser 195 from His 57 well beyond hydrogen-bonding proximity. Superposition is centred on Asp 102.

Table 1 Data processing, refinement and models

Crystals	
Space group	C222$_1$
Cell dimensions (Å)	$a = 63.2$; $b = 171.3$; $c = 145.8$
Solvent content (%)	49.2
Data processing statistics	
Wavelength (Å)	0.87 (Daresbury SRS, station 9.6)
Resolution (Å)	42.3/2.6
Total reflections	190,117
Unique reflections	24,548
$\langle I/\sigma(I)\rangle$	4.3
$\langle I\rangle/\sigma(\langle I\rangle)$	12.0
Completeness (%)	99.2
Multiplicity	7.7
R_{merge}	0.158
Model	
Number of protein/water residues	567/56
Residues modelled	
α_1-antitrypsin	Asn^{24}–Met^{358}, Ser^{359}–Lys^{394}
trypsin	Cys^{42}–Ser^{61}, Ala^{85}–Lys^{109}, Ile^{121}–Ile^{138}, Cys^{157}–Leu^{185}, Cys^{191}–Lys^{222}, Pro^{225}–Asn^{245}
Average B-factor (Å^2)	43.8
Refinement statistics	
Reflections in working/free set	23,506/1,042
R-factor/R_{free}	20.5/23.9
r.m.s. deviation of bonds (Å)/ angles (°) from ideality	0.0064/1.37
Ramachandran plot; residues in	
most favoured region (%)	85.7
additionally allowed region (%)	13.6
generously allowed region (%)	0.7
disallowed region (%)	0

the tetrahedral transition state. We conclude that this disruption is a direct consequence of the limited length of the serpin reactive-centre loop, which causes the plucking of the ester-linked Ser 195 away from its catalytic partners. The nonspecific nature of this mechanism explains how a single member of the serpin family can inhibit several serine proteases. The serpin–protease interface is limited with only two major contacts expected to contribute to the stability of the complex: Lys 328 of α_1-antitrypsin forms a salt-bridge with the conserved trypsin Asp 194 (Fig. 3c), and Asn 314 forms three hydrogen bonds with main-chain carbonyl oxygens in trypsin. These interactions are not specific to trypsin and should aid in the stabilization of the complex between α_1-antitrypsin and any chymotrypsin family member.

The imposed distortion of Ser 195 is directly linked to further distortions and loss of order in the rest of the complexed trypsin molecule. One important contribution is the associated movement of Asp 194 to form a new interaction with Lys 328 of α_1-antitrypsin (Fig. 3c) while breaking its salt bridge with the free amino group of Ile 16. In trypsinogen, where the amino group of Ile 16 is masked by the propeptide, a region known as the activation domain is disordered but becomes ordered upon activation to trypsin[4]. The activation domain, which comprises residues from the amino terminus to 19, 142–152, 184–193 and 216–223, accounts for about a third of the portion of trypsin that becomes disordered or distorted in the complex with α_1-antitrypsin. By breaking the interaction involving Asp 194, the serpin reverses the zymogen activation mechanism. Further distortions may be transmitted from Ser 195 through the series of disulphide bridges in trypsin. The disordered region also includes the calcium-binding site. Although each of these perturbations will contribute to the overall disruption of trypsin, the most significant factor is likely to be the steric clash due to the forced overlap with the serpin (Figs 1, 2 and Supplementary Information). The protease is, in effect, crushed against the body of the serpin. This explains why the serpins have evolved so that the energy released upon loop insertion results in a

molecule that is hyperstable, whereas the protease, as with most other proteins, has evolved to be just stable enough to prevent unfolding at ambient temperatures. Thus, the challenge of the steric overlap of the two structures leaves the α_1-antitrypsin unaffected, but results in a substantial collapse of the ordered structure of trypsin.

The relevance of the mechanism of inhibition presented here to the serpins in general is supported by studies on a variety of serpin–protease complexes using fluorescence, proteolysis and NMR[5,6,10,11,17–19]. Their collective results outline the changes observed here, but the field has remained unconvinced[20,21]. With the determination of the crystal structure of the complex these controversies can now be put to rest, but we are also aware that the structure opens further questions and new opportunities for research. One small, but obvious, question has already been answered by an experiment of nature. Is the limited length of the reactive-centre loop of the serpin a critical factor in the distortion of the catalytic triad and hence the stability of the complex? An incidental test of this was reported in a study of a family with a bleeding disorder[22]. The disorder was caused by the insertion of an extra residue into the reactive-centre loop of the fibrinolysis inhibitor α_2-antiplasmin. The tightness of the tethering to the serpin reactive-centre loop is therefore a critical factor in causing the distortion of the protease that leads to inhibition. Thus, serpins inhibit serine proteases by a novel mechanism, a fifth example to add to the four recently listed by Bode and Huber[23]—inhibition by deformation. □

Methods

The complex of N-terminally histidine-tagged human α_1-antitrypsin and bovine pancreatic trypsin (Sigma) was formed at pH 7 by incubation for 3 h at room temperature using a 2.9-fold molar excess of α_1-antitrypsin over trypsin. The reaction was stopped by the addition of 4-(2-aminoethyl)benzenesolfonyl fluoride (Sigma) to 1 mM, and cooling on ice. The complex was purified using a pH gradient from 5.7 to 8.0 on a Poros S column (PerSeptive Biosystems, Framingham, Massachusetts), and concentrated to 10 mg ml^{-1} in 20 mM NaAcetate, pH 5.7. Crystals were obtained from hanging drops containing 0.2 M

tri-NaCitrate and 20% PEG 3350, at a final pH of 7.4 (PEG/Ion Screen, Hampton Research, San Diego, California) within two weeks at 4 °C. Intact complex was verified by SDS–polyacrylamide gel electrophoresis of washed crystals (see Supplementary Information). Data were collected from a single frozen crystal, cryoprotected in 28.5% PEG 4000 and 10% PEG 400, at beamline 9.6 at the SRS Daresbury, UK.

The data were processed using MOSFLM[24] and merged using SCALA[25] from the CCP4 package[26] (Table 1) The molecular replacement solution for α_1-antitrypsin in the complex was obtained using AMORE[27] and the structure of cleaved α_1-antitrypsin[28] as the search model. Conventional molecular replacement searches failed to place a model of intact trypsin[29] in the complex, although maps calculated with phases from α_1-antitrypsin alone showed clear density for the ordered portion of trypsin (Fig. 3 and Supplementary Information). It was immediately apparent that density was only present for about half of the volume expected to be occupied by intact trypsin. A search model comprising trypsin residues 27–124 and 230–245 was orientated using AMORE to compute a domain rotation function[30] against structure factors corresponding to a sphere of the ordered density, which were calculated using the program GHKL (L. Tong, unpublished data). The position of the oriented model relative to α_1-antitrypsin was determined with AMORE using the original diffraction data. The entire model of trypsin was superimposed on the fragment and then truncated to the limits of the electron density to provide an initial model of the complex. The truncated model, to our surprise, was nearly complete in accounting for the ordered structure contributing to the diffraction data, despite including only about 50% of the trypsin residues. In fact, the amount of ordered density changed little throughout the course of refinement. Completeness of this model was estimated at 99% by a σ_A-plot computed in the program SIGMAA[31]. The model comprising α_1-antitrypsin alone was estimated to be 83% complete, whereas α_1-antitrypsin comprises only 62% of the mass of the complex (σ_A-plots are included as Supplementary Information). The final molecular model was achieved through an iterative procedure of rebuilding using XtalView and refinement in CNS[32] using a maximum likelihood target[33]. Statistics for data processing, refinement and for the final model are given in Table 1. Figures were made using the programs Molscript[34], Bobscript[35] and Raster3D[36].

1. Potempa, J., Korzus, E. & Travis, J. The serpin superfamily of proteinase inhibitors: structure, function, and regulation. *J. Biol. Chem.* **269**, 15957–15960 (1994).
2. Laskowski, M. & Qasim, M. A. What can the structures of enzyme-inhibitor complexes tell us about the structures of enzyme substrate complexes? *Biochim. Biophys. Acta* **1477**, 324–337 (2000).
3. Loebermann, H., Tokuoka, R., Deisenhofer, J. & Huber, R. Human alpha 1-proteinase inhibitor. Crystal structure analysis of two crystal modifications, molecular model and preliminary analysis of the implications for function. *J. Mol. Biol.* **177**, 531–557 (1984).
4. Huber, R. & Bode, W. Structural basis of the activation and action of trypsin. *Acc. Chem. Res.* **11**, 114–122 (1978).
5. Kaslik, G., Patthy, A., Balint, M. & Graf, L. Trypsin complexed with alpha 1-proteinase inhibitor has an increased structural flexibility. *FEBS Lett.* **370**, 179–183 (1995).
6. Stavridi, E. S. *et al.* Structural change in alpha-chymotrypsin induced by complexation with alpha 1-antichymotrypsin as seen by enhanced sensitivity to proteolysis. *Biochemistry* **35**, 10608–10615 (1996).
7. Huber, R. & Carrell, R. W. Implications of the three-dimensional structure of alpha 1-antitrypsin for structure and function of serpins. *Biochemistry* **28**, 8951–8966 (1989).
8. Elliott, P. R., Abrahams, J. P. & Lomas, D. A. Wild-type alpha 1-antitrypsin is in the canonical inhibitory conformation. *J. Mol. Biol.* **275**, 419–425 (1998).
9. Wright, H. T. & Scarsdale, J. N. Structural basis for serpin inhibitor activity. *Proteins* **22**, 210–225 (1995).
10. Stratikos, E. & Gettins, P. G. Formation of the covalent serpin–proteinase complex involves translocation of the proteinase by more than 70 Å and full insertion of the reactive center loop into beta-sheet A. *Proc. Natl Acad. Sci. USA* **96**, 4808–4813 (1999).
11. Fa, M. *et al.* The structure of a serpin-proteinase complex revealed by intramolecular distance measurements using donor-donor energy migration and mapping of interaction sites. *Structure* **8**, 397–405 (2000).
12. Picard, V., Marque, P. E., Paolucci, F., Aiach, M. & Le Bonniec, B. F. Topology of the stable serpin–protease complexes revealed by an autoantibody that fails to react with the monomeric conformers of antithrombin. *J. Biol. Chem.* **274**, 4586–4593 (1999).
13. Carrell, R. W. & Owen, M. C. Plakalbumin, alpha 1-antitrypsin, antithrombin and the mechanism of inflammatory thrombosis. *Nature* **317**, 730–732 (1985).
14. Stein, P. E. *et al.* Crystal structure of ovalbumin as a model for the reactive centre of serpins. *Nature* **347**, 99–102 (1990).
15. Engh, R. A., Huber, R., Bode, W. & Schulze, A. J. Divining the serpin inhibition mechanism: a suicide substrate 'spring'? *Trends Biotechnol.* **13**, 503–510 (1995).
16. Gooptu, B. *et al.* Inactive conformation of the serpin alpha(1)-antichymotrypsin indicates two-stage insertion of the reactive loop: implications for inhibitory function and conformational disease. *Proc. Natl Acad. Sci. USA* **97**, 67–72 (2000).
17. Herve, M. & Ghelis, C. Conformational stability of the covalent complex between elastase and alpha 1-proteinase inhibitor. *Arch. Biochem. Biophys.* **285**, 142–146 (1991).
18. Olson, S. T. *et al.* Role of the catalytic serine in the interactions of serine proteinases with protein inhibitors of the serpin family. Contribution of a covalent interaction to the binding energy of serpin–proteinase complexes. *J. Biol. Chem.* **270**, 30007–30017 (1995).
19. Plotnick, M. I., Mayne, L., Schechter, N. M. & Rubin, H. Distortion of the active site of chymotrypsin complexed with a serpin. *Biochemistry* **35**, 7586–7590 (1996).
20. Gils, A. & Declerck, P. J. Structure-function relationships in serpins: current concepts and controversies. *Thromb. Haemost.* **80**, 531–541 (1998).
21. Harrop, S. J. *et al.* The crystal structure of plasminogen activator inhibitor 2 at 2.0 Å resolution: implications for serpin function. *Struct. Fold Des.* **7**, 43–54 (1999).
22. Holmes, W. E. *et al.* Alpha 2-antiplasmin Enschede: alanine insertion and abolition of plasmin inhibitory activity. *Science* **238**, 209–211 (1987).
23. Bode, W. & Huber, R. Structural basis of the endoproteinase-protein inhibitor interaction. *Biochim. Biophys. Acta* **1477**, 241–252 (2000).
24. Leslie A. W. G. in *Joint CCP4 and ESF-EACMB Newsletter on Protein Crystallography* vol. 26 (Daresbury Laboratory, Warrington, 1992).
25. Evans P. R. in *Proceedings of the CCP4 Study Weekend. Data Collection and Processing* (eds Sawyer, L., Isaacs, N. & Bailey, S.) 114–122 (Daresbury Laboratory, 1993).
26. Collaborative Computational Project Number 4. The CCP4 suite: programs for protein crystallography. *Acta Crystallogr.* **50**, 760–763 (1994).
27. Navaza, J. AMORE - An automated package for molecular replacement. *Acta Cryst. A* **50**, 157–163 (1994).
28. Engh, R. *et al.* The S variant of human alpha 1-antitrypsin, structure and implications for function and metabolism. *Protein Eng.* **2**, 407–415 (1989).
29. Lee, S. L. New inhibitors of thrombin and other trypsin-like proteases: hydrogen bonding of an aromatic cyano group with a backbone amide of the P1 binding site replaces binding of a basic side chain. *Biochemistry* **36**, 13180–13186 (1997).
30. Colman, P. M., Fehlhammer, H. & Bartles, K. in *Crystallographic Computing Techniques* (eds Ahmed, F. R., Huml, K. & Sedlacek, B.) 248–258 (Munksgaard, Copenhagen, 1976).
31. Read, R. J. Improved Fourier coefficients for maps using phases from partial structures with errors. *Acta Cryst. A* **42**, 140–149 (1986).
32. Brunger, A. T. *et al.* Crystallography & NMR system: A new software suite for macromolecular structure determination. *Acta Cryst. D* **54**, 905–921 (1998).
33. Pannu, N. S. & Read, R. J. Improved structure refinement through maximum likelihood. *Acta Cryst. A* **52**, 659–668 (1996).
34. Kraulis, P. J. MOLSCRIPT: a program to produce both detailed and schematic plots of protein structures. *J. Appl. Crystallogr.* **24**, 946–950 (1991).
35. Esnouf, R. Further additions to MolScript version 1.4, including reading and contouring of electron-density maps. *Acta Crystallogr. D* **55**, 938–940 (1999).
36. Merritt, E. A. & Bacon, D. J. Raster3D: photorealistic molecular graphics. *Methods Enzymol.* **277**, 505–524 (1997).

•••

errata

Intraprotein radical transfer during photoactivation of DNA photolyase

Corrine Aubert, Marten H. Vos, Paul Mathis, André P. M. Eker & Klaus Brettel

Nature **405,** 586–590 (2000).

Figure 5 of this paper contained an error. The lower right-hand box in the reaction scheme, which read 'FADH⁻ TrpH TrpH TrpH˙', should have read 'FADH⁻ TrpH TrpH Trp˙'. ☐

Neural synchrony correlates with surface segregation rules

Miguel Castelo-Branco, Rainer Goebel, Sergio Neuenschwander & Wolf Singer

Nature **405,** 685–689 (2000).

In Fig. 1b of this Letter, the scale bar for the repetitive fields should be half as large as it was printed. In Fig. 1c, the label that reads PMLS should read A18. ☐